Detailed analysis of vibrational nonequilibrium of molecular oxygen in shock-heated flow

Iain D. Boyd*
Department of Aerospace Engineering, University of Michigan, Ann Arbor, Michigan 48109, USA

Eswar Josyula†
U.S. Air Force Research Laboratory, Wright-Patterson Air Force Base, Ohio 45433, USA
(Received 7 September 2017; published 18 December 2017)

A detailed comparison is made of two different methods for simulating vibrational relaxation behind a strong shock wave in molecular oxygen. The first approach is phenomenological and makes a number of strong assumptions in using an overall vibrational energy relaxation equation. The second approach resolves all of the quantized vibrational energy states using temperature-dependent state-to-state transition rates. Comparisons with experimental measurements indicate that the state-resolved approach is more accurate. The assumptions made in the phenomenological model are assessed in detail by using the state-resolved approach. It is determined that all of the assumptions made in the simpler model are violated directly behind a strong shock wave. A parameter based on the effects of multi-quantum transitions is proposed for predicting when the more detailed modeling approach must be used in compressed non-reacting flows and is found to be effective.

DOI: 10.1103/PhysRevFluids.2.123401

I. INTRODUCTION

Hypersonic vehicles fly at Mach numbers exceeding 5. When the high-speed flow interacts with the vehicle, a strong shock wave is formed that generates very high temperatures. These high temperatures lead to activation of the vibrational energy modes of the molecules and eventually to dissociation chemistry. The distribution of energy among the available energy modes and the chemical composition of the gas have significant effects on the heat transferred from the hot gas to the vehicle. Indeed, protection of a hypersonic vehicle against the high rates of heat transfer is one of the primary design drivers for these systems.

Due to the high costs and technical challenges associated with ground and flight testing of hypersonic systems, computer simulation and modeling plays a key role in the design of hypersonic vehicles. It is therefore important that the models employed in computer simulations are able to accurately capture all of the relevant flow physics processes.

Over the years, there has been a significant body of research conducted to understand the thermochemical processes in high-temperature air that are relevant to the extreme hypersonic conditions at Mach 25 associated with re-entry into Earth's atmosphere from space. Much of that work is summarized by Park [1]. There has been much less study of the thermochemistry of hypersonic flow associated with lower Mach numbers in the range of 5 to 15, and most of the work has concentrated on molecular nitrogen (N_2) that constitutes about 80% of air by volume (see, e.g., Panesi *et al.* [2] and Kim and Boyd [3]). To address an important gap, the focus of the present study is on the vibrational relaxation of molecular oxygen (O_2). While O_2 only represents about 20% of air, its weaker internal structure means that it becomes vibrationally activated more easily than nitrogen, and it dissociates more readily than nitrogen. Thus, there are some hypersonic flow conditions where most of the thermochemistry concerns oxygen.

*iainboyd@umich.edu
†eswar.josyula@us.af.mil

The primary objective of the current study is to predict when a widely used phenomenological model for oxygen thermochemistry, the so-called two-temperature model [1], provides predictions that are sufficiently accurate. There are many potential aspects of the problem to consider: compressed and expanded flows; energy transfer to the rotational, vibrational, and electronic energy modes; and chemical reactions. As a starting point, the current study is deliberately limited to vibrational energy transfer in compressed flows in order to try and establish a firm foundation on which further work can build. The objective of assessing the validity of the phenomenological model is addressed through the use of a more detailed approach that fully resolves all of the quantum vibrational states of molecular oxygen in a simulation.

The structure of the article is as follows: First, a description is provided of oxygen shock-tube experiments that provide test conditions and measurements to provide context for the modeling results. Then, the phenomenological and state-resolved modeling approaches are described. Results are then presented in which the models are compared with the experiments, and further analyses are performed to understand the sources of the differences in the solutions obtained. The article ends with a summary and conclusions.

II. THERMOCHEMISTRY MODELING

In the present work, the upstream conditions are first used to determine the immediate post normal shock state using the jump conditions derived from the Rankine–Hugoniot relations [4]. It is assumed that the vibrational energy modes and chemistry are all frozen across the shock wave. The electronic energy modes are neglected throughout. In reality, a shock wave has a finite thickness of several mean free paths corresponding to a distance on the order of 0.01 cm for the conditions studied. This distance is a very small fraction (about 0.5%) of the total domain sizes considered. Omitting the details of the shock front is therefore considered to have a negligible effect on the results presented. Numerical simulation capabilities are then employed for the analysis of the shock tube flow downstream of the shock. In these simulations, the one-dimensional, inviscid (Euler) equations of fluid flow are solved. The standard Euler conservation equations are augmented by additional equations to describe the nonequilibrium thermochemistry. Two-temperature (2T) and state-to-state (STS) approaches are employed to model the thermochemistry.

In the 2T model [1], it is assumed that a single temperature T describes the translational and rotational energy modes of the gas, and a separate temperature T_v describes the vibrational mode. Two energy equations are solved: one for the total energy (which includes all energy modes), and one for the vibrational mode. The focus of this study is on vibrational relaxation, and in the 2T model this process is described by the Landau–Teller (LT) equation [5],

$$\frac{dE_v}{dt} = \frac{E_v^*(T) - E_v(t)}{\tau_v}, \tag{1}$$

where $E_v(t)$ is the total vibrational energy at time t, $E_v^*(T)$ is its equilibrium value at temperature T, and τ_v is the vibrational relaxation time that is usually evaluated as

$$\tau_v = \tau_{MW} + \tau_P, \tag{2}$$

with the first term due to Millikan and White [6]. The second term, a high-temperature correction due to Park [7], has the following form:

$$\tau_p = \frac{1}{n\sigma_v C}, \tag{3a}$$

where n is the total number density, and C is the average thermal speed. The vibrational cross section is given by Park [7] is

$$\sigma_v = 3 \times 10^{-21}\left(\frac{50\,000}{T}\right)^2. \tag{3b}$$

The most important and explicit assumptions of the LT equation are [8]

(1) The vibrational energy distributions are in the equilibrium Boltzmann form.

(2) The relaxation process is characterized by a single relaxation time τ_v.

(3) There are also implicit assumptions underlying the LT equation that allow one to construct an equivalent state-to-state approach:

(4) The vibrational energy spacing is constant (simple harmonic oscillator, SHO).

(5) Only single quantum transitions are allowed, $\Delta v = \pm 1$.

(6) Using these assumptions, it may be shown [8] that the equivalent de-activation transition rate from the first to the ground vibrational level is related to the overall vibrational relaxation time by

$$K_{1,0} = \frac{1}{\tau_v[1 - \exp(-\theta_v/T)]}, \tag{4}$$

where θ_v is the characteristic temperature for vibration, and T is the gas dynamic temperature. Further analysis leads to the result that all of the equivalent deactivation and activation rates consistent with the LT model are related to the relaxation time through the $K_{1,0}$ deactivation rate [8]:

$$K_{i+1,i} = (i+1)K_{1,0} \quad \text{and} \quad K_{i,i+1} = (i+1)K_{1,0}\exp(-\theta_v/T). \tag{5}$$

In the analysis of oxygen in the current study, the standard approach described above using Eqs. (2), (3a), and (3b) is employed for O_2-O_2 relaxation because it is known to be accurate. For O_2-O relaxation, an overall vibrational relaxation time derived from a recent, detailed computational chemistry analysis [9] is employed; it was shown to be more accurate than the standard result obtained from Eqs. (2), (3a), and (3b).

While the focus of the present study is on vibrational relaxation, it is useful to briefly describe the 2T approach for simulating chemical nonequilibrium. A separate continuity equation is solved for each chemical species in the flow. The chemical source terms are evaluated using kinetic rate equations in which the rate coefficients are evaluated as a function of temperature in modified Arrhenius form. The oxygen dissociation rates employed in the present study are those given by Park [7]. For dissociation reactions, the controlling temperature in the rate coefficients is taken as the geometric mean of the translational and vibrational temperatures. It is further assumed that a certain amount of energy is subtracted from the vibrational energy mode due to each dissociation collision. This energy is often characterized as some fixed fraction of the dissociation energy with 0.45 being a common value that is used in the present analysis.

The STS approach provides a much more detailed description of thermochemical nonequilibrium by solving a separate continuity equation for each of the quantized vibrational energy states, the so-called master equation approach. Thus, each quantized state is treated as a separate chemical species. There is no longer a need to solve a separate vibrational energy equation with the master equation approach. In the present implementation, all possible quantum state transitions Δv are included in the evaluation of the source term for each vibrational state. The bound-bound (non-dissociation) transition rates for O_2-O_2 collisions are evaluated by using the semi-analytical forced harmonic oscillator model [10]. The important potential energy parameter employed in the forced harmonic oscillator model in the present work is $\alpha = 4.0\,\text{Å}^{-1}$. For O_2-O interactions, the transition rates are taken from detailed analysis that employed quasi-classical trajectory (QCT) simulations [9]. The potential energy surfaces used in these rate models provide for 47 anharmonic vibrational energy states for the oxygen molecule. The QCT-derived analysis includes rate coefficients for both bound-bound (energy transfer) and bound-free (dissociation chemistry) interactions. Again, while the focus of the current study is on bound-bound transitions, it is necessary to briefly describe how bound-free (dissociating) transitions are handled. For O_2-O_2, the QCT dissociation rates of for O_2-O are scaled to match the overall dissociation rate recommended by Bortner [11]. For O_2-O, the QCT rates of Ref. [9] are employed directly.

III. RESULTS AND ANALYSIS

A. Thermochemical nonequilibrium analysis

Shock-tube flows represent the simplest configuration for study that are also accessible to experimental investigation. Current shock-tube simulations are performed on a uniform mesh of 1000 nodes covering 2 cm of physical space. The upstream temperature is 295 K, the velocity is chosen to achieve a downstream temperature of interest, and the pressure is chosen to ensure that the vibrational relaxation process is completed within a distance of 2 cm. The first case considered has a pressure of 10 torr, and a velocity of 2.03 km/s that equates to a Mach number of 6.2 and an equilibrium downstream temperature of about 2100 K. At the post-shock conditions, the degree of dissociation of molecular oxygen is about 0.25%.

Figure 1(a) compares the translational and vibrational temperature profiles obtained for the Mach 6.2 case by using the LT and STS approaches. In the simulation, the dissociation chemistry is negligible and is therefore disabled. Under these conditions, there is very good agreement between the two simulations. Figure 1(b) shows vibrational energy distribution functions (VEDFs) as symbols obtained from the STS simulation at three different locations downstream of the shock. In each case, the Boltzmann distribution corresponding to the same total vibrational energy is included as a solid line and these appear as straight lines on this semi-log plot. There is some non-Boltzmann behavior immediately after the shock, but in general the distributions are close to being equilibrium Boltzmann.

The second shock-tube condition chosen corresponds to that of an experiment conducted in pure oxygen by Ibraguimova *et al.* [12]. Reference [12] reports the use of absorption spectroscopy to determine the vibrational temperature of O_2 as a function of distance behind the shock wave. While a number of different cases are presented in Ref. [12], for the purposes of the present study, attention is focused on the weakest shock generated under the following conditions upstream of the shock wave: a pressure of 2.0 torr, a temperature of 295 K, and a velocity of 3.07 km/s, representing a Mach number of 9.4. This weakest case is selected to minimize the effects of dissociation chemistry on the vibrational energy mode. Figure 2(a) shows temperature profiles including the vibrational temperature measurements. In this case, the dissociation chemistry modeling is included in the simulations, and so the solution that employs the LT model for vibrational relaxation and Park's two-temperature model for dissociation is labeled "2T." A logarithmic scale is used with distance to more clearly show the details of the profiles. There is considerable scatter in the experimental measurements with both models providing profiles that overlap with most of the measured data. Using the experimental data only up to the point where the vibrational temperature reaches a maximum, at about 0.3 cm behind the shock (after which effects of chemistry become non-negligible), the standard deviations of the experimental data from the 2T and STS solutions are 14.5% and 9.8%, respectively. The overall experimental uncertainty in each data point is $\pm 10\%$. Therefore, the STS approach provides results that are closer to the experimental data and within the experimental uncertainty. Figure 2(b) shows the species mole fractions indicating that this is indeed a weakly dissociating case, and the mole fraction of atomic oxygen is about 3% at the location of the maximum value of the vibrational temperature.

B. Thermal nonequilibrium analysis

The primary objective in this study is to determine the conditions under which the more detailed, state-to-state treatment of vibrational nonequilibrium is required in place of the LT model. Therefore, for the remainder of this study, the second case is analyzed in the absence of dissociation chemistry, for which the LT and STS temperature profiles are shown in Fig. 2(c). Note that both sets of predictions overpredict the measured vibrational temperature in the downstream region due to the omission of dissociation chemistry, which removes energy from all energy modes. Unlike the results shown in Fig. 1(a), under these stronger shock conditions, there is a significant difference between the LT and STS solutions.

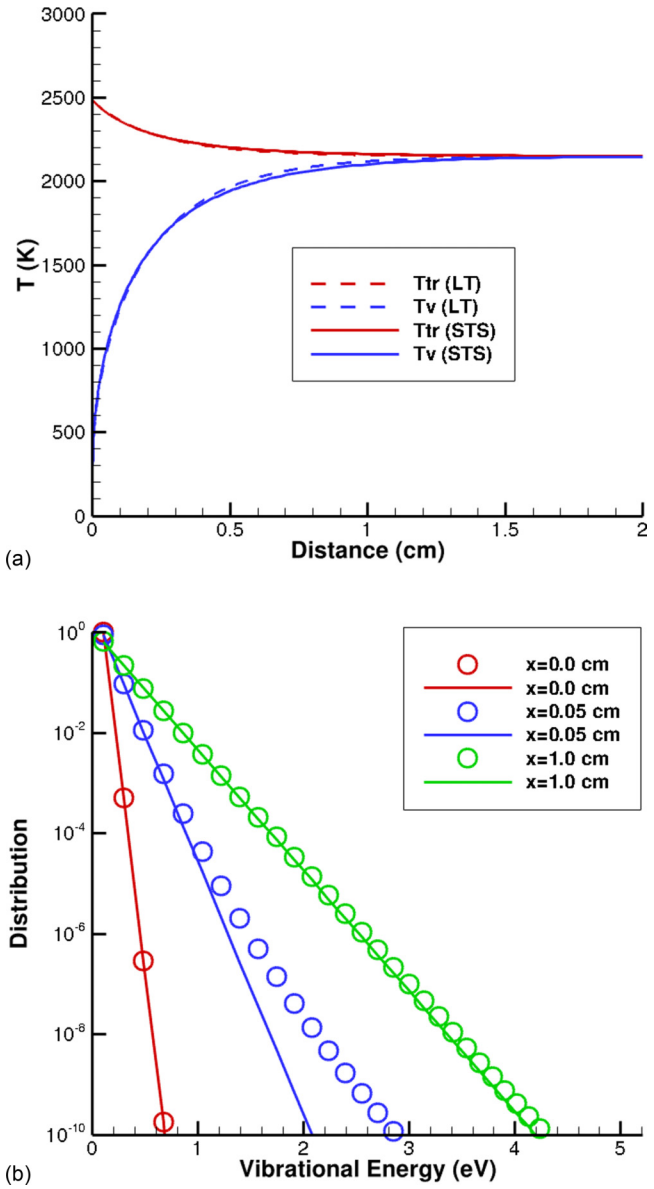

FIG. 1. (a) Profiles of temperature in a Mach 6.2 shock wave of oxygen. (b) Vibrational energy distributions from the STS model in a Mach 6.2 shock wave of oxygen. Note: Solid lines are shown to demonstrate the deviation from a Boltzmann distribution.

The question of predicting when the STS approach is needed for accurate results can be considered from two perspectives: (1) use the LT results to predict when the STS approach is required; and (2) use the STS results to predict when the LT approach is adequate.

We begin with the first approach. Figure 3 shows profiles of a number of different local Knudsen numbers evaluated from the LT solution. In each case, the local Knudsen number is defined as [13]

$$Kn_X = \lambda \left| \frac{1}{X} \frac{dX}{dx} \right|, \tag{6}$$

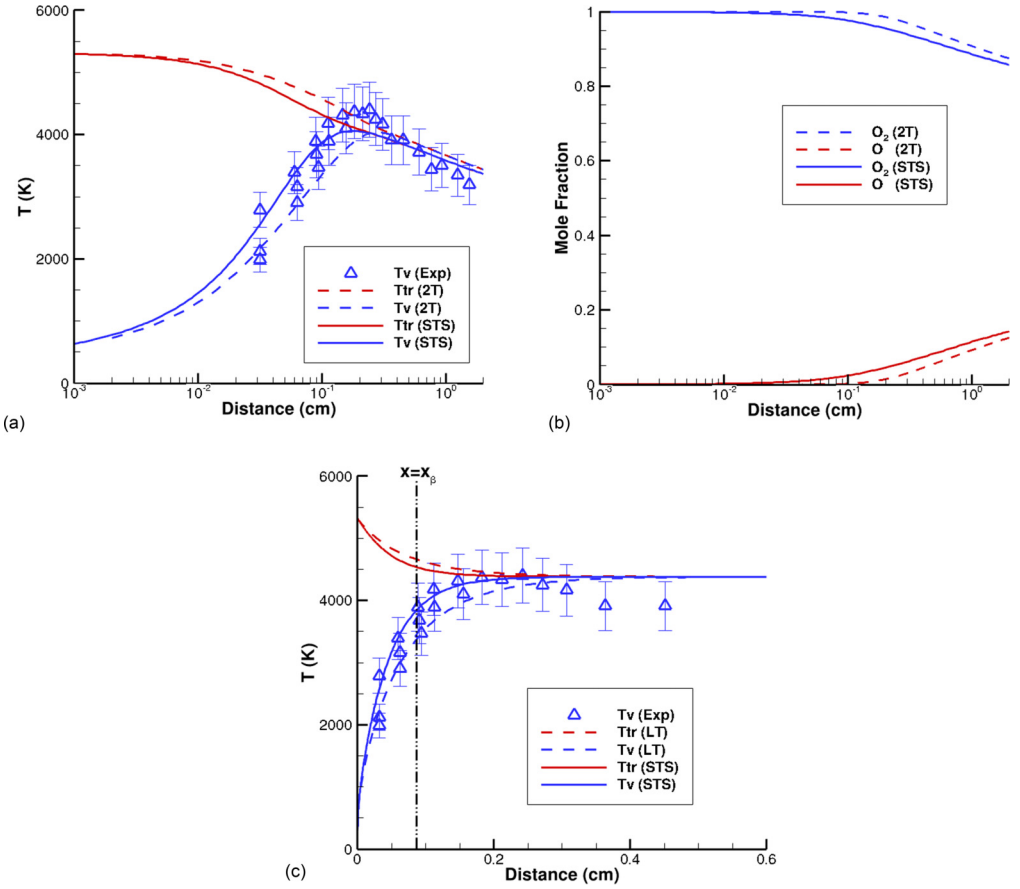

FIG. 2. (a) Profiles of temperature in a Mach 9.4 shock wave of oxygen including dissociation chemistry. (b) Profiles of mole fraction in a Mach 9.4 shock wave of oxygen including dissociation chemistry. (Mole fraction = 0.03−0.06 at $x = 0.3$ cm). (c) Profiles of temperature in a Mach 9.4 shock wave of oxygen neglecting dissociation chemistry.

where X is a flow property (density, velocity, translational temperature, vibrational temperature), λ is the local mean free path, and x is distance. A value of this parameter exceeding 0.05 indicates that the flow is in the translational nonequilibrium regime in which the continuum approximation is invalid [13]. The Knudsen numbers based on gas dynamic properties (density, translational temperature, velocity) are all similar and show initial values immediately downstream of the shock front that are less than 0.05, and that subsequently decrease strongly further behind the shock. The local Knudsen numbers associated with vibrational temperature are initially much higher indicating stronger levels of nonequilibrium behavior. The corresponding results from the STS profiles are similar to those obtained from the LT solutions and neither of them immediately suggests a way to determine when the STS approach is required.

Another approach to characterizing nonequilibrium involves comparison of the characteristic flow time τ_f with the characteristic relaxation time of a thermochemical process, τ_p [14]. These characteristic times are defined as follows:

$$\tau_f = \frac{\Delta x}{u} \quad \text{and} \quad \tau_p = \frac{1}{u}\left|\frac{1}{X}\frac{dX}{dx}\right|^{-1}, \tag{7}$$

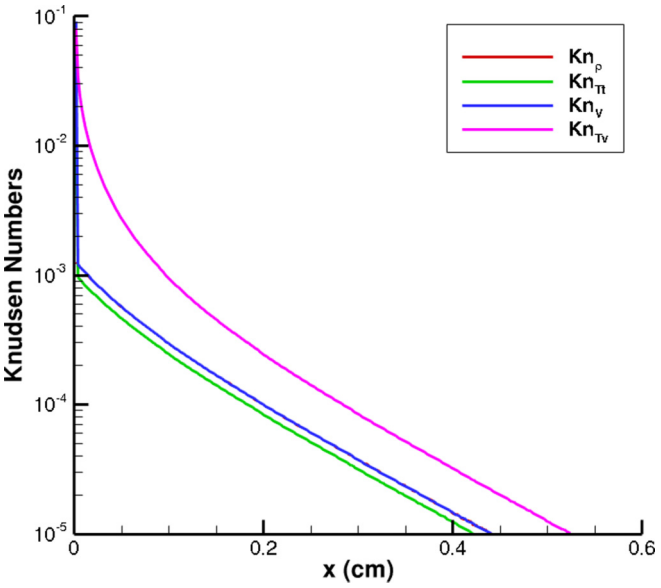

FIG. 3. Profiles of local Knudsen number from the LT solution.

where u is the flow velocity. For our focus on vibrational relaxation, X is set to the vibrational temperature. Nonequilibrium is indicated whenever $\tau_f/\tau_p < 1$ as in this case the relaxation process cannot reach its end state before the flow variables change. Figure 4 shows the profile of the ratio of the characteristic flow time to the characteristic time for vibrational relaxation obtained from the LT solution. The post-shock region displays vibrational nonequilibrium. The corresponding profiles obtained from the STS solution are similar. While this parameter indicates that there is vibrational

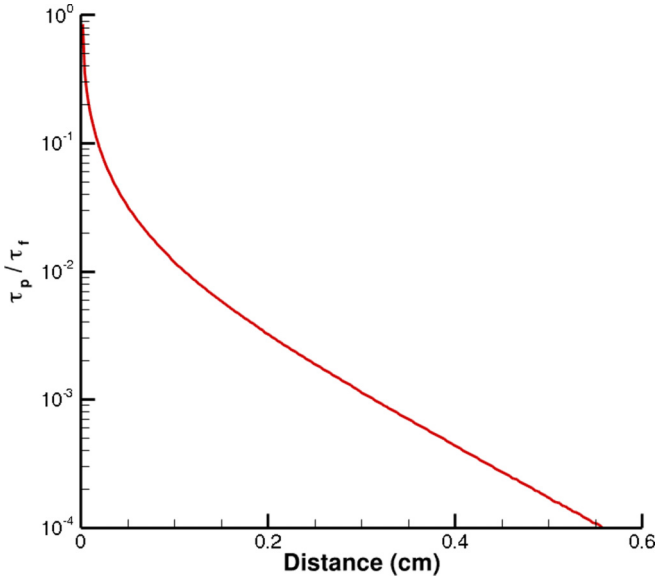

FIG. 4. Profile of the ratio of characteristic times from the LT solution.

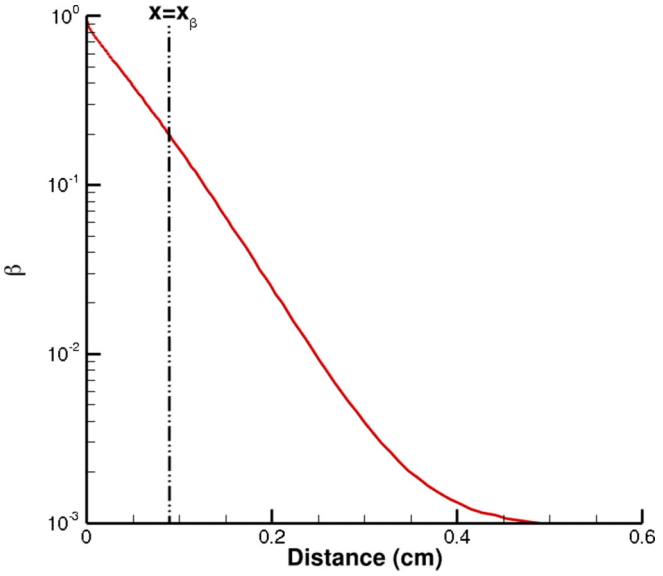

FIG. 5. Profile of the temperature difference criterion [15] from the STS solution.

nonequilibrium in this flow, it does not provide information on whether the LT or STS approach is required for accurate simulation.

It is perhaps not surprising that using the LT solution to predict its own inadequacies is not successful. Therefore, we now consider the second approach of using the state-resolved solution to predict when the LT approach is sufficiently accurate. Recently, Burt and Josyula [15] proposed the following *temperature difference criterion* for detection of regions of near-equilibrium vibrational processes in a flow field:

$$\beta \equiv \frac{|T_v - T|}{T}, \tag{8}$$

where T is the translational-rotational temperature and T_v is the vibrational temperature given by

$$T_v = \frac{\varepsilon_1 - \varepsilon_0}{k \ln(f_0/f_1)}, \tag{9}$$

in which ε_0 and ε_1 are the vibrational energies of the ground and first excited states, respectively, k is Boltzmann's constant, and f_0 and f_1 are the population fractions of the ground state and first-excited state, respectively. Figure 5 shows the profile of β evaluated from the STS solution for the Mach 9.4 shock wave of oxygen with dissociation disabled. Reference [15] suggests that a value of $\beta > 0.2$ indicates regions of vibrational nonequilibrium where the full STS treatment is required, although it is not a universal number. Based on this criterion, Fig. 5 suggests that only the region of about 0.088 cm immediately downstream of the shock requires full STS treatment.

However, Fig. 2(c) shows that the STS solution provides improved agreement with the experimental data than the LT approach over a much larger region of physical space. Figure 2(c) also shows that the region of space for which there is significant difference between the LT and STS solutions is much larger than the first 0.088 cm behind the shock. Therefore, the β parameter is not successful in predicting when the detailed approach is needed for this particular case.

To fully understand the differences in the results provided by the STS and the LT models, the fundamental assumptions in the LT approach are assessed in detail using the STS results. From our

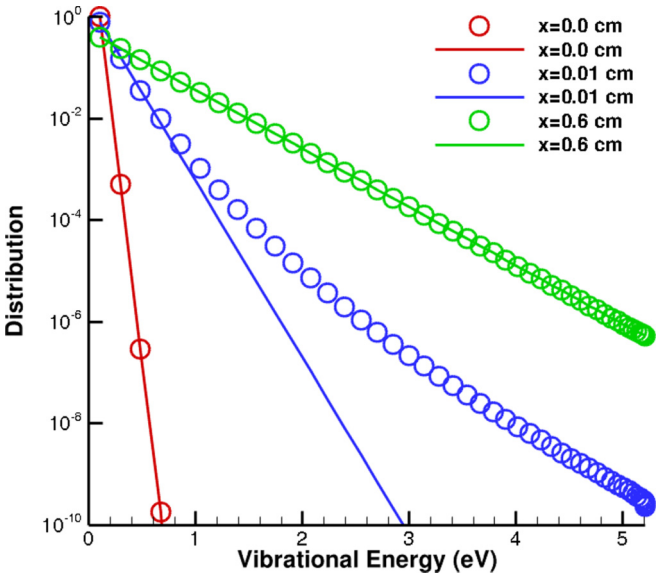

FIG. 6. Vibrational energy distributions from the STS model in a Mach 9.4 shock wave of oxygen. Note: Solid lines are shown to demonstrate the deviation from a Boltzmann distribution.

earlier discussion, the most important assumptions of the LT vibrational relaxation model are the following:

(1) The vibrational energy distributions are in the equilibrium Boltzmann form.
(2) The relaxation process is characterized by a single relaxation time τ_v.
(3) The vibrational energy spacing is constant (SHO).
(4) Only single quantum transitions are allowed $\Delta v = \pm 1$.
(5) The equivalent de-activation transition rate from the first to the ground vibrational level is related to the overall vibrational relaxation time by Eq. (4).
(6) The equivalent deactivation and activation rates consistent with the LT model are related to the relaxation time through $K_{1,0}$ and Eq. (9).

To assess the first assumption of the LT model that the vibrational mode is described by equilibrium distributions, Fig. 6 shows the VEDFs as symbols obtained from the STS simulation at three different locations downstream of the shock. Again, in each case, the Boltzmann distribution corresponding to the same total vibrational energy is included as a solid line and these appear as straight lines on this semi-log plot. The results show that there is a region in the first 0.01 cm behind the shock where the VEDF is non-Boltzmann and so the first assumption of the LT model is violated. The upper levels are significantly overpopulated in comparison to the equivalent Boltzmann distribution. From the Mach 9.4 shock, the first appearance of non-Boltzmann behavior is at a probability of about 0.01 whereas, for the Mach 6.2 case shown in Fig. 1(b), the non-Boltzmann behavior first occurs at a lower probability of about 0.001. Hence, for the stronger shock, the effect of non-Boltzmann VEDFs is more pronounced. It is conjectured that the over-population of the upper levels occurs due to the monotonic decrease in the quantum energy spacing for a real anharmonic oscillator that makes it easier for activation to occur in the upper levels. Of course, this effect would be reduced when dissociation is included in the analysis since these reactions tend to occur preferentially from the upper vibrational levels. In any case, part of the explanation for the differences between the LT and STS solutions is the fact that the region immediately after the shock contains strongly nonequilibrium vibrational energy distributions.

To assess the combination of assumptions (2) through (4), Fig. 7 compares the $K_{1,0}$ and $K_{0,1}$ rates as a function of temperature for O_2-O_2 obtained from the vibrational relaxation time employed in

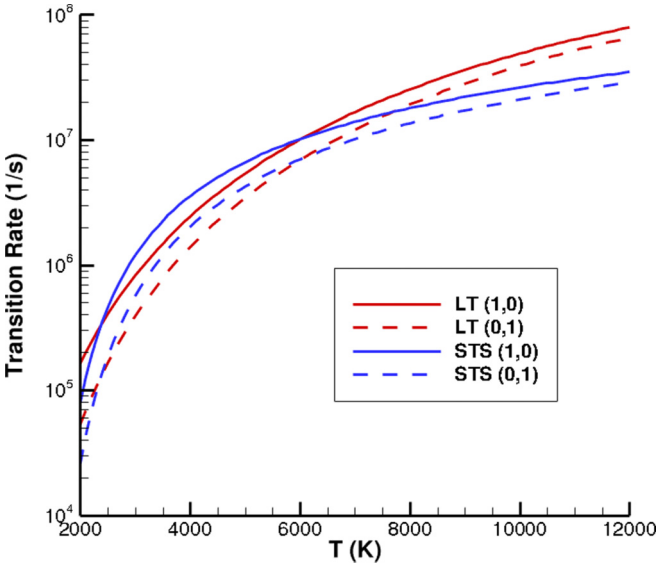

FIG. 7. Transition rates as a function of temperature for the LT and STS models.

the LT model based on Eqs. (8) and (9) with the rates employed in the STS approach. For analysis of the increase in vibrational temperature immediately behind a shock, we are most interested in the activation rates, and it is seen that the LT model predicts a lower rate than STS for the temperature range immediately behind the shock in Fig. 2(c). This lower activation rate is partially responsible for the lower vibrational temperatures predicted by the LT model in comparison to the STS approach. However, the difference in $K_{0,1}$ rates is only about 25% and when the LT rates are artificially increased by this amount, achieved by decreasing τ_v by 25%, the resulting vibrational temperatures shown in Fig. 8 still lie below the STS values. Thus, a second reason for the differences in the LT and STS solutions is that, if there is an overall relaxation time, it is not the same between the two models.

To further explicitly assess the fourth assumption of the LT model, Fig. 9 shows the temperature dependence of the ratio:

$$\Delta \equiv \frac{K_{0,1}}{\sum_{i=1}^{i-\max} K_{0,i}},$$

in which the rates are evaluated by using those employed in the STS calculations. Under the fourth assumption of the LT model, Δ should have a value of 1.0 indicating that multi-quantum transitions are negligible. As expected, Fig. 9 shows that the importance of multi-quantum transitions increases with temperature. For the conditions immediately behind the shock, as shown in Fig. 2(c), the value of Δ lies in the range 0.92–0.95. To further assess the fourth assumption, Fig. 10 shows temperature profiles obtained with the STS approach in which only single quantum transitions are included. The new profile offers close agreement with the LT profile in Fig. 9 obtained with the relaxation time decreased by 25%.

To further isolate the effects of nonequilibrium, another analysis is conducted using the state-to-state approach in which only single quantum transitions are allowed for vibrational energy levels specified by the SHO, and where the transition rates are evaluated from the overall vibrational relaxation time using Eqs. (4) and (5). Note that there are only 27 evenly space vibrational energy levels with the SHO model for oxygen. Figure 11(a) compares the temperature profiles obtained from this STS-SHO approach with the full STS results, and with the experimental measurements. The STS-SHO profile is very similar to that obtained with the LT approach shown in Fig. 2(c). Some

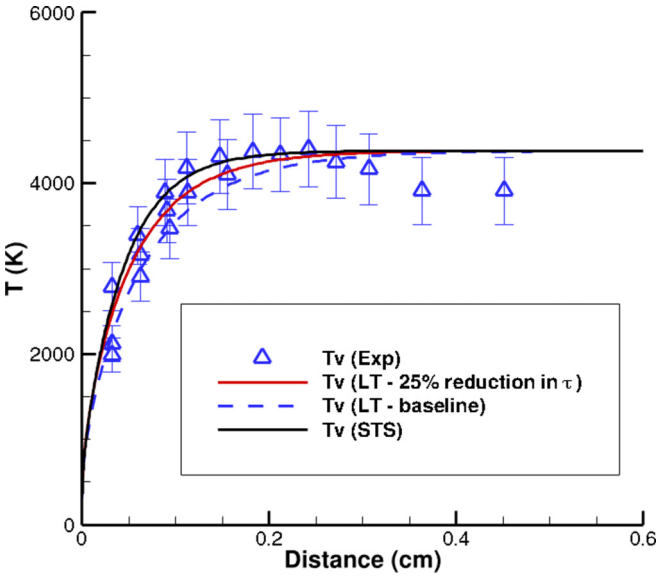

FIG. 8. Temperature profiles in the Mach 9.4 shock with dissociation disabled: Effect of reduction in relaxation time used in the LT approach.

of the vibrational energy distributions obtained with the STS-SHO model are shown in Fig. 11(b). As expected from theory [8], the VEDFs in this model progress through a series of Boltzmann energy distributions. These results indicate that the LT approach is effective at reproducing the results obtained by the more detailed, but still inaccurate, STS-SHO model. By comparison with the STS VEDFs from Fig. 6, it is also clear that vibrational nonequilibrium is missing from the STS-SHO approach.

These analyses indicate that the STS results show behavior immediately behind the shock wave that is inconsistent with all four major assumptions in the LT model for vibrational relaxation.

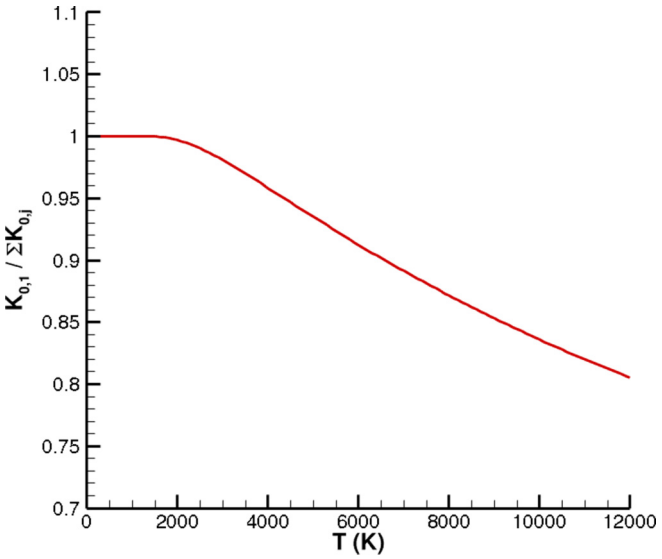

FIG. 9. Temperature dependence of a parameter that indicates the significance of multi-quantum transitions in the STS model.

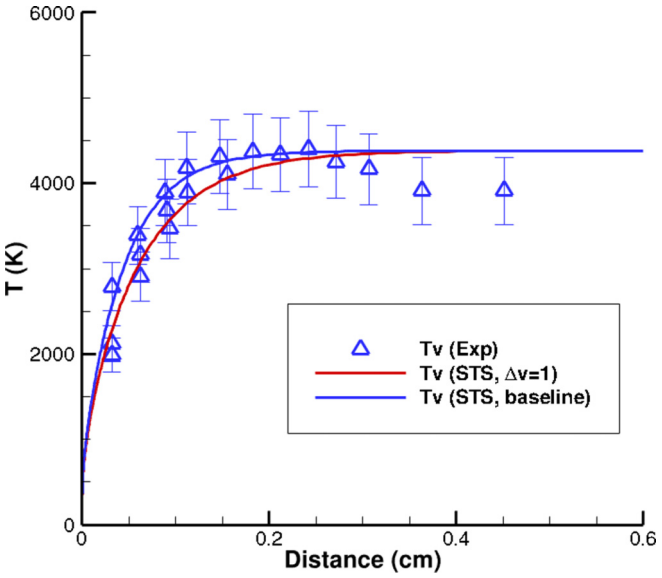

FIG. 10. Temperature profiles for the Mach 9.4 shock from the STS solution with dissociation disabled: Effect of restricting $\Delta v = 1$.

Furthermore, in not making these restrictive assumptions, the STS approach produces different results that are in better agreement with the available measurements. The question remains about how to predict when the STS approach is required based on the flow conditions. One problem with the parameter of Burt and Josyula [15] is that it appears to be very conservative. For example, for the conditions upstream of the shocks investigated experimentally in Ref. [12], this parameter indicates that any shock creating a translational temperature behind the shock in excess of about 369 K will result in $\beta > 0.2$. Such a temperature is created by a very weak shock wave with a Mach number of 1.4, for which the detail of the STS model is certainly unnecessary.

A better approach is to use a parameter based on the analyses presented above of the conditions for which the assumptions of the LT model are invalid. The most important aspect that is missing from the LT model is the effect of multi-quantum transitions that become important above a certain temperature. From Fig. 9, if we use a 1% effect from multi-quantum transitions as the point at which the detailed approach is required, then this behavior occurs at temperatures above 2500 K. For an upstream temperature of 295 K, that temperature is reached immediately downstream of a Mach 6.2 shock wave in oxygen. The solutions for these conditions was already presented in Figs. 1(a) and 1(b). Clearly, the profiles from the LT and STS approaches are indeed in good agreement. It is therefore concluded that the temperature dependence of the Δ parameter can be used to predict when the STS approach is required. For oxygen, a cutoff temperature of 2500 K is recommended. The cutoff temperature must be determined by the unique vibrational relaxation characteristics of each molecular gas.

C. Summary and Conclusions

The present study focused on a Mach 9.4 shock-tube case in pure oxygen that mainly involved vibrational relaxation with low levels of molecular dissociation. Results were obtained with the phenomenological Landau–Teller (LT) model and with a state-to-state (STS) approach that resolved the vibrational energy distribution function. The experimental results for this case had a lower standard deviation from the STS results than from the LT results. Further detailed analysis of this case indicated that the STS model predicted nonequilibrium vibrational energy distribution functions

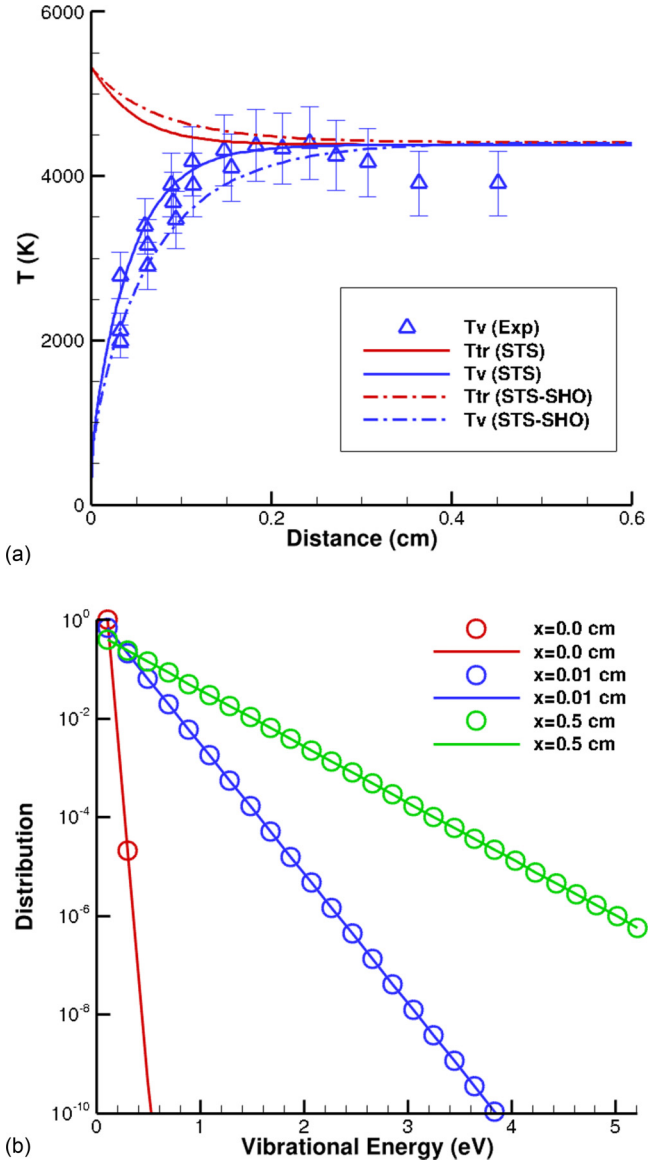

FIG. 11. (a) Temperature profiles for the Mach 9.4 shock with dissociation disabled including the solution for SHO energy levels and $\Delta v = \pm 1$ rates from the overall vibrational relaxation time (labeled STS-SHO). (b) Vibrational energy distributions from the solution for SHO energy levels and $\Delta v = \pm 1$ rates from the overall vibrational relaxation time (STS-SHO). Note: Solid lines are shown to demonstrate the deviation from a Boltzmann distribution.

(VEDFs) and that multi-quantum transitions have a significant effect. Both of these features are missing from the LT approach.

A number of different parameters were evaluated for potential prediction of when the more detailed physics of the STS approach would be required in order to obtain physically accurate results for vibrational energy transfer in non-reacting compressed flows. The most useful parameter appears to be one based on quantification of the significance of the effects of multi-quantum transitions.

For the Mach 9.4 shock wave of the experiment, this parameter correctly indicated that the detailed approach is needed. For Mach numbers of 6.2 and less in oxygen, the parameter indicated that the two-temperature approach should be sufficient. This prediction was confirmed through direct comparison between STS and LT solutions.

In future work, an analysis will be performed of stronger shock cases in oxygen investigated experimentally in Ref. [12] in which the effects of dissociation chemistry on the vibrational energy will be significant. Once again, the goal will be to determine a parameter that can successfully predict when detailed STS analysis is required. In addition, analyses will be conducted for other important gases such as N2 and NO to determine the cutoff temperature for use of the STS approach based on the effects of multi-quantum transitions.

---

[1] C. Park, *Nonequilibrium Hypersonic Aerothermodynamics* (Wiley, New York, 1989).

[2] M. Panesi, R. L. Jaffe, D. W. Schwenke, and T. E. Magin, Rovibrational internal energy transfer and dissociation of $N_2(1\sum g+) - N(4Du)$ system in hypersonic flows, J. Chem. Phys. **138**, 044312 (2013).

[3] J. G. Kim and I. D. Boyd, Master equation analysis of post normal shock waves of nitrogen, J. Thermophys. Heat Trans. **29**, 241 (2015).

[4] K. Neitzel, D. A. Andrienko, and I. D. Boyd, Aerothermochemical nonequilibrium modeling for oxygen flows, J. Thermophys. Heat Trans. **31**, 634 (2017).

[5] L. Landau, and E. Teller, Theory of sound dispersion, Physikalische Zeitschrift der Sowjetunion **10**, 34 (1936).

[6] R. C. Millikan and D. R. White, Systematics of vibrational relaxation, J. Chem. Phys. **39**, 3209 (1963).

[7] C. Park, J. T. Howe, R. L. Jaffe, and G. V. Candler, Review of chemical kinetic problems of future NASA missions, I: Earth entries, J. Thermophys. Heat Trans. **7**, 385 (1993).

[8] W. G. Vincenti and C. H. Kruger, *Introduction to Physical Gas Dynamics* (Krieger Press, Miramar, 1986).

[9] D. A. Andrienko and I. D. Boyd, Rovibrational energy transfer and dissociation inO_2-O collisions, J. Chem. Phys. **144**, 104301 (2016).

[10] I. V. Adamovich, S. O. Macheret, J. W. Rich, and C. E. Treanor, Vibrational relaxation and dissociation behind shock waves. Part 2: Master equation modeling, Am. Inst. Aeronaut. Astronaut. J. **39**, 1916 (2001).

[11] M. Bortner, A review of rate constants of selected reactions of interest in re-entry flow fields in the atmosphere. tech, National Bureau of Standards, U.S. Dept. of Commerce TR Note 484 (1969).

[12] L. Ibraguimova, A. Sergievskaya, and O. Shatalov, Dissociation rate constants for oxygen at temperatures up to 11 000 K, Fluid Dyn. **48**, 550 (2013).

[13] I. D. Boyd, G. Chen, and G. V. Candler, Predicting failure of the continuum fluid equations in transitional hypersonic flows, Phys. Fluids **7**, 210 (1995).

[14] I. D. Boyd and T. E. Schwartzentruber, *Nonequilibrium Gas Dynamics and Molecular Simulation* (Cambridge University Press, New York, 2017).

[15] J. M. Burt and E. Josyula, Vibrational nonequilibrium quantification for state-resolved simulation of a hypersonic flow, J. Thermophys. Heat Trans. **31**, 660 (2017).